Fixation of distal fibular fractures:
A biomechanical study of plate fixation techniques

Jiri Marvan[1], Zdenek Horak[2]*, Miloslav Vilimek[3],
Lukas Horny[3], David Kachlik[2, 5], Vaclav Baca[2, 4]

[1] Department of Orthopedics and Traumatology, Third Faculty of Medicine, Charles University,
Ruska 87, 10000 Prague, Czech Republic.
[2] College of Polytechnics Jihlava, Tolsteho 16, 58601 Jihlava, Czech Republic.
Tel.: (+420) 604 128 156, e-mail: zdenek.horak@vspj.cz
[3] Department of Mechanics, Biomechanics and Mechatronics, Faculty of Mechanical Engineering, Czech Technical University,
Technicka 4, 16607 Prague, Czech Republic.
[4] Department of Anatomy, Third Faculty of Medicine, Charles University, Ruska 87, 10000 Prague, Czech Republic.
[5] Department of Anatomy, Second Faculty of Medicine, Charles University, V Uvalu 84, 15006 Prague, Czech Republic.

Ankle fractures are complex injuries with variable prognoses that depend upon many factors. The aim of the treatment is to restore the ankle joint biomechanical stability with maximum range of motion. Most ankle fractures are fibular fractures, which have a typical oblique fracture line in the distal fibula located in the area of the tibiofibular syndesmosis. The aim of this study was to simulate numerically several fixation techniques of the distal fibular fractures, evaluate their stability, determine their impact on surrounding tissue load, and correlate the results to clinical treatment experience. The following three models of fibular fracture fixation were used: (a) plate fixation with three screws attached above/below and lag screws, (b) plate fixation with two screws attached above/below and lag screws, and (c) three lag screws only. All three fracture fixation models were analyzed according to their use in both healthy physiological bone and osteoporotic bone tissue. Based on the results of Finite Element Analysis for these simulations, we found that the most appropriate fixation method for Weber-B1 fibular fractures was an unlocked plate fixation using six screws and lag screws, both in patients with physiological and osteoporotic bone tissue. Conversely, the least appropriate fixation method was an unlocked plate fixation with four screws and lag screws. Although this fixation method reduces the stress on patients during surgery, it greatly increased loading on the bone and, thus, the risk of fixation failure. The final fixation model with three lag screws only was found to be appropriate only for very limited indications.

Key words: *fibular fracture, finite element analysis, osteosynthesis, fracture fixation, fibula*

1. Introduction

Ankle fractures are complex injuries with variable prognosis that depends upon many factors such as fracture type, bone tissue quality, character of ligamentous lesions, treatment technique, biological status of the patient, associated injuries, and complications [3], [4], [19], [21]. According to statistics from the Department of Orthopedics and Traumatology, ankle fractures are ranked in third place after fractures of the distal radius and proximal femur [13].

The aim of the treatment is to restore ankle joint biomechanical stability with maximum range of motion. The Weber's, AO, and Lauge-Hansen's classifications are most commonly used in clinical practice [21], [22]. Ankle fractures in a group of patients surgically treated at Department of Orthopedics and Traumatology consisted of Weber-A (5%), Weber-B (72%) and Weber-C (23%) types. Ankle joint stability is a crucial factor when deciding upon conservative or surgical treatment. Fibular fracture type (Weber-A, -B, or -C) is a decisive treatment factor and exact restoration of fibula length, shape, and position in the

tibiofibular syndesmosis is a fundamental requirement. Exact treatment of all ankle joint structures [10] is essential to ensure good results; however, our paper will focus on the lateral part of the ankle and the important task of proper reconstruction of the fractured distal fibula.

The most common cases include Weber-B1 fractures that have a typical oblique fracture line in the distal fibula located in the area of the tibiofibular syndesmosis. Most of them are stabilized with either 3.5 mm-long lag (compression) screws, or a one-third neutralization plate (independently, or as a lag screw supplement). Biomechanical stability of the structure with lag screw only fixation must be accompanied by immobilizing plaster fixation, because it is clinically considered less stable. Use of one-third fixation plates enables earlier treatment function of the structure. Advantages of the lag screw only method include reduced soft tissue dissection, reduced prominence of osteosynthetic material under the skin, reduced pain on the lateral side of the ankle, and a reduced need to remove screws and plate. In theory, a smaller incision with less metallic material should result in less soft tissue irritation and reduced risk of infection. In practice, plate osteosynthesis for distal fibular fractures (one-third tubular plate) usually involves three screws inserted above and below the fracture. When using locking compression plates (LCP) (which have the advantage of being indicated for osteoporotic bone and extensive comminuted fragments), the literature describes the introduction of two locked screws above and below the fracture zone as adequate [13], [16].

When respecting the aforementioned rules in traumatology practice, the issue of selecting the appropriate technique arises. On the one hand, it is a relatively less stable structure (lag screws only) with the undisputed advantages of a minimally invasive approach, reduced prominence of metallic material under the skin, and an expected reduction of wound healing complications [5], [15]. On the other hand, an osteosynthesis plate is a stable solution associated with potentially early rehabilitation of the ankle joint without the need for a plaster cast [1]. Stabilization of fibula fractures without plaster cast using shorting time for full patient recovery, decreases muscle atrophy and patient discomfort. This led us to the experimental study described below which examines the basic stability parameters of stress and stiffness in the area where osteosynthetic material is introduced into bone. To correlate clinical experience from treating distal fibular fractures in everyday practice with information from literary sources, we wanted to obtain data and conclusions pertaining to the stability of individual types of osteosynthesis of the distal fibula in an experimental plane. The numerical simulations used were optimal for comparison of the different fractures fixation. Numerical simulations were more appropriate than the experimental tests realized on cadavers or synthetic bone models. Next reasons for using numerical simulations were repeatability, time demands and financial costs.

2. Materials and methods

Parametric FEM simulations of loading on fixed fibular fractures were performed using the ABAQUS program (Dassault Systèmes, France). The finite element method (FEM) was the optimum method for performing these tasks [8], [9], [17], [20] and it has a long tradition in biomechanics and clinical medicine. The aim of these analyses was to determine the response of the model system to external loading and compare three fibular fracture fixation techniques that are commonly used in clinical practice. The following models of the Weber-B fibular fracture fixation [3], [4] were evaluated: (a) plate fixation with three screws inserted above and below and lag screws (Model A3); (b) plate fixation with two screws inserted above and below and lag screws (Model A2); and (c) three lag screws only (Model B) (Fig. 1). All three models analyzed were consistent with clinical practice and only the posterior tibiofibular ligament was modeled; the anterior tibiofibular ligament and the interosseous tibiofibular ligament were regarded as having ruptured, and the interosseous membrane of the leg as being intact.

The geometric 3D model of the ankle joint was created from CT scans of healthy individuals with no apparent injuries or degenerative changes on bone. The images were formed at a resolution of 512×512 pixels, with pixel size of 0.424 mm, and 0.75 mm spacing of individual cuts. Geometric reconstruction of individual ankle joint components was performed using the MIMICS program (Materialise, Belgium). The resultant 3D geometric model was subsequently imported into the Rhinoceros program (Robert McNeel & Associates, Washington, USA) and a Weber-B1 fibular fracture was created on the basis of a real clinical case. The fracture was fixed in cooperation with clinical experts and according to conventional clinical practice.

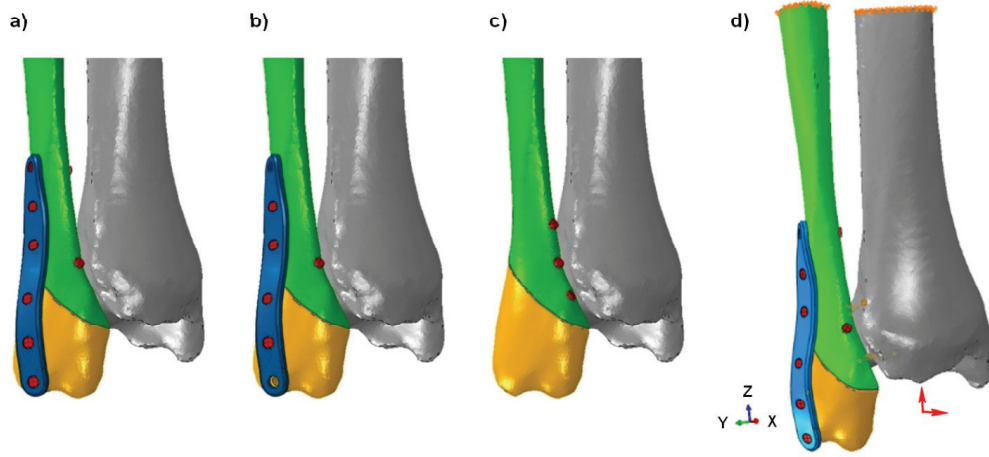All numerical FE analyses for plate and screw fixation used an isotropic, homogeneous elasto-plastic

Fig. 1. Analyzed models of ankle joints with fixed fibular fractures: (a) Model A3, (b) Model A2,
(c) Model B, and (d) model with boundary condition, applied forces and coordinate system

material model ($E = 210$ GPa, $\nu = 0.3$, $\sigma_y = 690$ MPa). Plate and screws were made from titanium alloy which has commonly been used for medical device for decades. Bone tissue was modeled as nonhomogeneous isotropic elasto-plastic material, where its material parameters were designated according to bone density $E = f(\rho)$ that was determined from CT scans. Methodologies presented in several papers [7], [11], [12] were used to determine material parameters. The simulations involved bone tissue crack at the moment its yield stress σ_y was exceeded. Density was determined based on shades-of-gray color in CT images of the distal femur and were calculated according to the ratio

$$\rho = 1.54 \cdot \rho_{CT} + 0.0784 \qquad (1)$$

where ρ_{CT} [g/cm^3] is the density of calibration sample. The moduli of elasticity E [MPa] for both types of bone tissue (compact and spongy) were determined using ratios [11], [12]

$$E^c = 2065 \cdot \rho^{3.09}; \quad v^c = 0.3, \\ E^s = 1904 \cdot \rho^{1.64}; \quad v^s = 0.3. \qquad (2)$$

The same method was used to determine the value of the yield point σ_y [MPa] as a function related to the value of bone tissue density according to [11], [12]

$$\sigma_y^c = 57.75 \cdot \rho^{1.73} \quad \text{for} \quad \rho \geq 0.945, \\ \sigma_y^s = 76.50 \cdot \rho^{6.70} \quad \text{for} \quad \rho < 0.945. \qquad (3)$$

In computational analyses, the bone tissue was also modeled as a material in which exceeding the loading limit leads to degradation of its mechanical properties. This property can, through transferred meaning, be understood as "damage" to bone tissue.

These modeled properties are best illustrated in Fig. 2, where a line graph shows the relationship between stress and deformation.
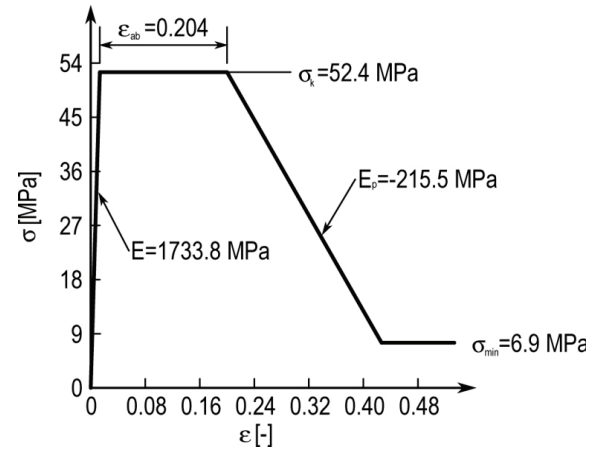

Fig. 2. Specification of material properties. Illustration of the relationship between stress σ [MPa] and strains ε [–] of bone tissue with density $\rho = 0.945$ [g/cm^3]

The individual values that unambiguously describe the behavior of the material model, when exceeding σ_y, were also determined in relation to the density of bone tissue ρ according to

$$\sigma_{\min} = 8.5 \cdot \rho^{3.68}; \quad \varepsilon_{ab} = 0.258 \cdot \rho - 0.04, \\ E_p = -244 \cdot \rho^{2.2}; \quad \varepsilon_{ab} = \left| \frac{\sigma_y - \sigma_{\min}}{E_p} + \varepsilon_{ab} \right|. \qquad (4)$$

All numerical tasks were modeled as nonlinear static problems, which were performed in the ABAQUS program. Fixation screws (Zimmer, cortical screws diameter 3.2 mm and cancellous screws diameter 4.0 mm) were meshed by linear 8-node elements with a global size

of 0.6 mm. The plate (Zimmer, one-third tubular plate) was meshed by quadratic 4-node element with global size of 0.75 mm. Bone tissue was meshed by linear 4-node element with a global size of 1.5 mm; at the point of contact with fixation screws, the mesh was locally changed to a size of 0.9 mm.

General contact with the friction coefficient $f = 0.3$ was modeled for all parts of the model [18]. Fixation screw heads were inserted into the plate and allowed free movement and the screws were preloaded with axial force of $F_0 = 2.5$ N. Fixation screws were inserted into bone tissue using coupling conditions that fix all nodal displacements on the screw surface with nodal displacements on the surface of the hole in the bone tissue. The posterior tibiofibular ligament was modeled using 1D Link-type connector elements that only had one degree of freedom. Ligament stiffness ($k = 128.8$ N.mm^{-1}) was determined experimentally. The free ends of the tibia and fibula were fixed by constrained node displacements and rotations in global coordinate system. The entire model was loaded with a force that corresponded to the maximum force applied to the ankle joint during walking. The magnitude of force corresponded to that of a 75 kg individual walking slowly. This reaction force ($F_z = 2056$ N and $F_y = -288$ N) was distributed to the articular surfaces of the ankle joint using distributed coupling condition. The same coupling condition was used to fix the posterior tibiofibular ligament to bone tissue wherein the insertion area size corresponded to the physiology of healthy individuals.

3. Results

The parametric FE analysis results are summarized in Table 1, Figs. 3 and 4. In order to evaluate individually analyzed models, a stiffness parameter [N.mm^{-1}] was introduced; it was defined as $k = F/u_{max}$, where F is the force acting on the ankle joint and u_{max} is the maximum displacement of the fibula during loading with force F. When comparing the overall stiffness of the ankle joint with a fixed fibular fracture model system, the most rigid model for physiological (subscript "f") and osteoporotic (subscript "p") bone tissue was Model A3 ($k_f = 400.9$ N.mm^{-1} and $k_p = 212.3$ N.mm^{-1}). In both types of bone tissue (physiological and osteoporotic), Model A2 was found to be 5.7% and 6.9% less rigid ($k_f = 377.9$ N.mm^{-1} and $k_p = 197.6$ N.mm^{-1}). Model B was the least rigid in both types of bone tissue ($k_f = 366.8$ N.mm^{-1} and $k_p = 184.6$ N.mm^{-1}), which was 8.5% and 13.0% less stable relative to Model A3.

The situation was different when fixation screw loading was evaluated; yield stress σ_y limit values were exceeded in all of the analyzed models, irrespective of bone tissue quality. Limit exceedance always occurred in a relatively small area; however, this situation represents a risk in terms of the reliability of fibular fracture fixation. The maximum values observed for reduced stress σ_{red} in the fixation screws for Model A3 were $\sigma_{red}^f = 645.0$ MPa and $\sigma_{red}^p = 752.4$ MPa. In Model A2, the maximum values were $\sigma_{red}^f = 745.1$ MPa and $\sigma_{red}^p = 762.0$ MPa. In Model B the maximum values were $\sigma_{red}^f = 667.7$ MPa and $\sigma_{red}^p = 755.7$ MPa. As expected, fixation screws experienced more loading in osteoporotic bone, during which the magnitude of the maximum reduced stress, relative to physiological bone tissue values, increased by 16.6% (Model A3), 2.2% (Model A2), and 13.2% (Model B).

During the evaluation of fibular tissue, the maximum reduced stress σ_{red} [MPa] value was monitored. The FE simulation results clearly show that the least degree of loading in bone tissue occurred in Model A3 ($\sigma_{red}^f = 77.5$ MPa and $\sigma_{red}^p = 94.2$ MPa). Bone tissue in Model B ($\sigma_{red}^f = 93.4$ MPa and $\sigma_{red}^p = 95.5$ MPa) was loaded 20.5% and 1.4% (respectively) more than was observed in Model A3. The greatest degree of loading in the fibula occurred in Model A2 ($\sigma_{red}^f = 116.3$ MPa and $\sigma_{red}^p = 122.1$ MPa), which was 50.1%

Table 1. Resultant maximum reduced stress values σ_{red} [MPa] and overall stiffness [N.mm^{-1}]
in the ankle using a fixed fibular fracture model

	σ_{red}^f [MPa]			k_f [N.mm^{-1}]	σ_{red}^p [MPa]			k_p [N.mm^{-1}]
	Fibula	Screw	Plate		Fibula	Screw	Plate	
Model A3	77.5	645.0	300.7	400.9	94.2	752.4	347.2	212.3
Model A2	116.3	745.1	259.5	377.9	122.1	762.0	321.2	197.6
Model B	93.4	667.7	N/A	366.8	95.5	755.7	N/A	184.6

Variants for physiological bone tissue are marked with a superscript f, and variants for osteoporotic bone tissue are marked with a superscript p.

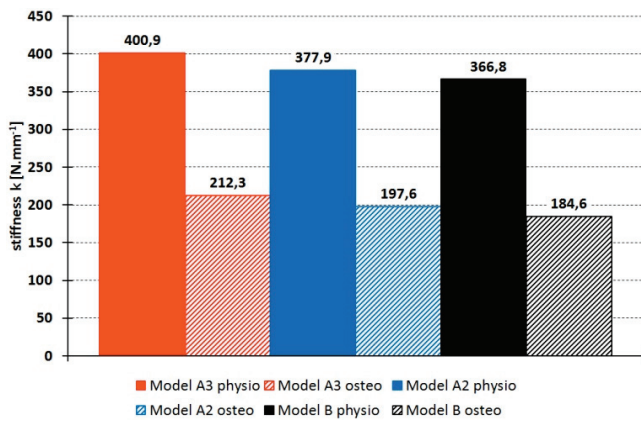and 29.6% (respectively) greater than was observed in Model A3.

Fig. 3. Graph depicting the degree of stiffness [N.mm^{-1}] for the entire model of the ankle joint with a fixed fibular fracture
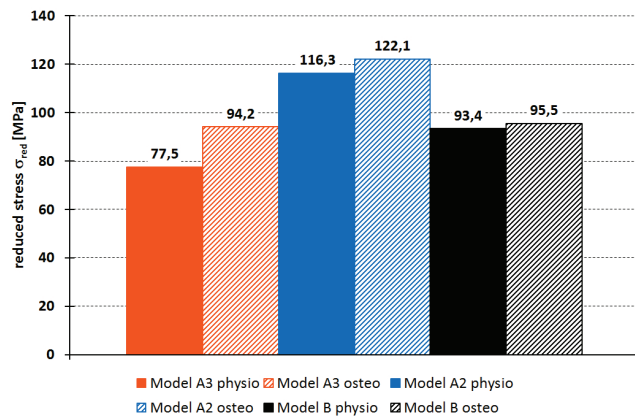

Fig. 4. Graph depicting the maximum degree of reduced stress σ_{red} [MPa] in the fibula
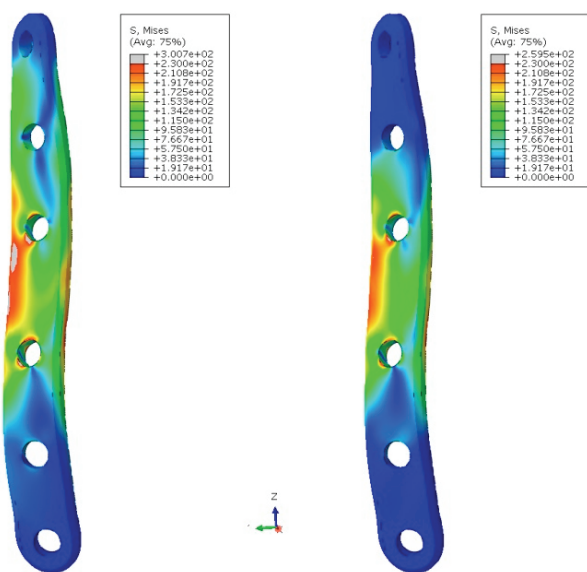

Fig. 5. Distribution of the reduced stress σ_{red} [MPa] in the plate for physiological bone: Model A3 (left) and Model A2 (right)
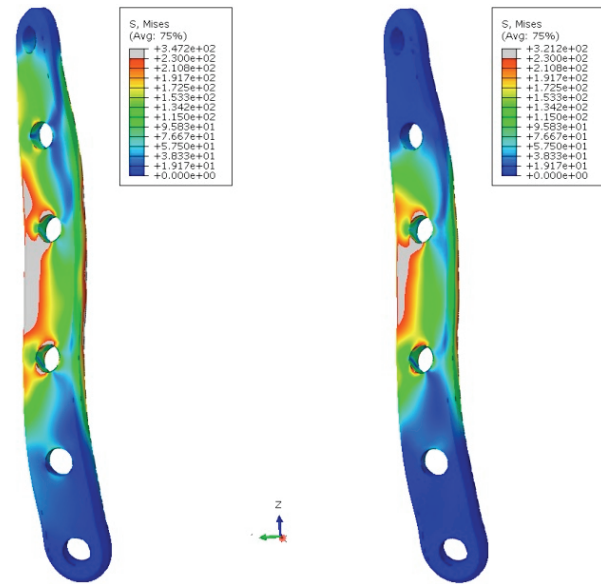

Fig. 6. Distribution of the reduced stress σ_{red} [MPa] in the plate for osteoporotic bone: Model A3 (left) and Model A2 (right)

The fixation plates did not exceed, or even approach the limits of, their material values in any of the analyzed models for either physiological or osteoporotic bone tissue. The maximum values observed for reduced stress σ_{red} in fixation plates in Model A3 were σ_{red}^{f} = 300.7 MPa and σ_{red}^{p} = 347.2 MPa, respectively (see Figs. 5 and 6). In Model A2, the maximum values were σ_{red}^{f} = 259.5 MPa and σ_{red}^{p} = 321.2 MPa, respectively. Based on the results obtained, it can be said that the fixation plate is sufficiently dimensioned with respect to its load and irrespective of the bone tissue quality.

4. Discussion

This paper presents the FE analysis results for three models of an ankle joint with a fixed fibular fracture. We evaluated three models that used three different fracture fixation techniques that are routinely used in clinical practice. Model A3 used an unlocked plate that was fixed to the bone in two locations (above the fracture and below the fracture) with three screws in each location and lag screws. Model A2 used an unlocked plate that was fixed to the bone in two locations with two screws in each location and lag screws. Model B used 3 lag screws only for fracture fixation. The primary FE analysis results pertained to the stiffness of the entire system and consequent stress applied to individual parts of the model. Loading of the model corresponded to a 75 kg patient walking slowly

with an injured ankle. All models used Weber-B1 fibular fractures, since it is one of the most common fractures encountered in clinical practice. Our FE analyses simulated both physiological and osteoporotic bone.

The resulting stiffness values of the modeled systems (Fig. 3) were consistent with study expectations and experience from clinical practice. For both physiological and osteoporotic bone tissue, the greatest stiffness was observed in Model A3, followed by Model A2, and the least stiffness was Model B; stiffness differences expressed as a percentage relative to Model A3 were 5.7% (Model A2) and 8.5% (Model B). Similar results for fracture fixation were also found in osteoporotic bone; stiffness differences expressed as a percentage relative to Model 3 were 6.9% (Model A2) and 13.0% (Model B). It is therefore evident that fracture fixation using three lag screws only (Model B) is only suitable in very limited patient indications (i.e., <55 years of age, very good bone tissue quality, and a simple fracture line). Conversely, and from a biomechanical perspective, the differences between the stiffness of Model A2 and Model A3 were relatively indistinguishable. Thus, it should also be possible to perform fixation with shorter, unlocked plates that have been fixed with two screws above and two screws below the fracture line, which could reduce surgical interventions and lead to faster patient recovery.

Nevertheless, when evaluating the stress on each individual model component, it is necessary to reassess the above results. Plate stress was almost the same in all analyzed cases and was not dependent on bone tissue quality. From this perspective, the structure appeared to be optimal and safe. However, the situation differed when assessing fixation screw loading; the yield stress $\sigma_y = 690$ MPa limit values were exceeded in all analyzed models (to the greatest extent in Model A2 at $\sigma_{\mathrm{red}}^{\mathrm{f}} = 745.1$ MPa and $\sigma_{\mathrm{red}}^{\mathrm{p}} = 762.0$ MPa). This finding particularly demonstrates the potential risk of fracture fixation failure in Model A2 compared to the lowest failure risk in Model A3 ($\sigma_{\mathrm{red}}^{\mathrm{f}} = 645.0$ MPa and $\sigma_{\mathrm{red}}^{\mathrm{p}} = 752.4$ MPa). Moreover, it is necessary to consider that the obtained results correspond to the situation immediately following bone fixation, at which time healing has not yet begun. During the course of bone tissue healing, a load redistribution occurs that results in reduced fixation screw stress. Nonetheless, from a biomechanical perspective, implementation of Model A2 in fibular fracture fixation is relatively risky.

However, we considered the most fundamental assessment to have been that of bone tissue loading due to fracture fixation. From this perspective, the least

degree of loading in both types of bone was observed in Model A3 ($\sigma_{\mathrm{red}}^{\mathrm{f}} = 77.5$ MPa and $\sigma_{\mathrm{red}}^{\mathrm{p}} = 94.2$ MPa). Conversely, the greatest degree of loading (irrespective of bone tissue quality) was observed in Model A2 ($\sigma_{\mathrm{red}}^{\mathrm{f}} = 116.3$ MPa and $\sigma_{\mathrm{red}}^{\mathrm{p}} = 122.1$ MPa). The increase in bone tissue loading relative to Model A3 was highly significant, with a 50.1% increase in physiological bone tissue and a 29.6% increase in osteoporotic bone tissue. An increase in bone tissue loading was also observed in Model B relative to Model A3, but to a lesser extent, with a 20.5% increase in physiological bone, and 1.4% in osteoporotic bone. The maximum reduced stress value σ_{red} at the point of fixation screw insertion was found for all models (i.e., the risk of screw loosening and failure of the fixation system). From a biomechanical perspective, these findings indicate that the least suitable fibular fracture fixation technique is an unlocked plate fixed at two locations with two fixation screws in each location.

The Finite Element Method has long been successfully used as a tool to assess the response of biological tissues and fixation materials to external loading [6], [2]. Nevertheless, it was necessary to use several simplifications, such as the use of coupling conditions to insert the fixation screws in bone tissue. This condition not only allowed the transmission of compressive forces, but also that of tensile forces that did not correspond to real situations in a threaded connection. This simplification was chosen due to the convergence and length of numerical simulations. In our opinion, these conditions did not reduce the validity of the results in any manner because the aim was to compare three different models under the same conditions (not to determine the absolute value of ankle joint loading). In this context, the results presented can be regarded as credible and objective.

We are aware that in some cases the fracture line in Weber-B fractures may not be long enough to apply one of the selected stabilization systems. The aim of our study was biomechanical modeling of each type of implant to find the most stable osteosynthesis for a standardized case. The limits in indication are marginally mentioned, because it is not the core of solutions of this study.

5. Conclusions

In closing, and from a biomechanical perspective, it can be concluded that the most appropriate fixation technique for Weber-B1 fibular fractures is the use of

an unlocked plate, fixed at two locations with three screws per location and lag screws. This conclusion applies to both physiological and osteoporotic bone. Conversely, the least suitable technique appears to be the use of an unlocked plate fixed at two locations with two screws per location and lag screws. Although this fixation technique reduces the load on patients during surgery, it increases the load on the bone and, thus, the risk of fixation failure. In terms of biomechanical properties, the final analyzed fracture fixation model that used three lag screws only, was found suitable for very limited indications.

Acknowledgment

Reference

[1] AKSAKAL B., GURGER M., SAY Y., YILMAZ E., *Biomechanical Comparison of Straight DCP and Helical plates for Fixation of Transverse and Oblique Bone Fractures*, Acta Bioeng. Biomech., 2014, 16, 67–74.

[2] AQUILINA P., CHAMOLI U., PARR W., CLAUSEN P., WROE S., *Finite element analysis of three patterns of internal fixation of fractures of the mandibular condyle*, Br. J Oral Maxillofac. Surg., 2013, 51, 326–331.

[3] ARASTU M.H., DEMCOE R., BUCKLEY R.E., *Current concepts review: ankle fractures*, Acta Chir. Orthop. Traumatol. Cech., 2012, 79, 473–483.

[4] BROWNER B., JUPITER J., KRETTEK C., ANDERSON P., *Skeletal Trauma: Basic Science, Management, and Reconstruction* (5 ed., Vol. 2). Elsevier Ltd., 2015.

[5] CARLILE G.S., GILES N.C., *Surgical technique for minimally invasive fibula fracture fixation*, Foot Ankle Surg., 2011, 17, 119–123.

[6] CRONSKÄR M., RASMUSSEN J., TINNSTEN M., *Combined finite element and multibody musculoskeletal investigation of a fractured clavicle with reconstruction plate*, Comput. Methods Biomech. Biomed. Engin., 2015, 18, 740–748.

[7] FAULKNER K., GLER C., GRAMPP S., GENANT H., *Cross-calibration of liquid and solid qct calibration standards: Corrections to the ucsf normative data*, Osteoporos. Int., 1993, 3, 36–42.

[8] HRUBINA M., HORAK Z., SKOTAK M., LETOCHA J., BACA V., DZUPA V., *Assessment of complications depending on the sliding screw position – finite element method analysis*, 2015, Bratisl. Lek Listy, 116, 302–310.

[9] JIRMAN R., HORAK Z., BOUDA T., MAZANEK J., REZNICEK J., *Influence of the method of TM joint total replacement implantation on the loading of the joint on the opposite side*, Comput. Methods Biomech. Biomed. Engin., 2011, 14, 673–681.

[10] KACHLIK D., BACA V., CEPELIK M., HAJEK P., MANDY'S V., MUSIL V., SKALA P., STINGL J., *Clinical anatomy of the retrocalcaneal bursa*, Surg. Radiol. Anat., 2008, 30, 347–353.

[11] KELLER T., *Predicting the compressive mechanical behavior of bone*, Journal of Biomechanics, 1994, 27, 1159–1168.

[12] KEYAK J., FALKINSTEIN Y., *Comparison of in situ and in vitro ct scan-based femoral fracture load*, Med. Eng. Phys., 2003, 25, 781–787.

[13] KIM T., AYTURK U.M., HASKELL A., MICLAU T., PUTTLITZ C.M., *Fixation of osteoporotic distal fibula fractures: A biomechanical comparison of locking versus conventional plates*, J. Foot Ankle Surg., 2007, 46, 2–6.

[14] MARVAN J., BELEHRADKOVA H., DZUPA V., BACA V., KRBEC M., *Epidemiological, morphological and clinical aspects of ankle fractures*, Acta Chir. Orthop. Traumatol. Cech., 2012, 79, 269–274.

[15] McKENNA P.B., O'SHEA K., BURKE T., *Less is more: lag screw only fixation of lateral malleolar fractures*, Int. Orthop., 2007, 31, 497–502.

[16] MILNER B.F., MERCER D., FIROOZBAKHSH K., LARSEN K., DECOSTER T.A., MILLER R.A., *Bicortical screw fixation of distal fibula fractures with a lateral plate: an anatomic and biomechanical study of a new technique*, J. Foot Ankle Surg., 2007, 46, 341–347.

[17] PAKULA G., SLOWINSKI J., SCIGALA K., *Biomechanics of distal femoral fracture fixed with an angular stable LISS plate*, Acta Bioeng. Biomech., 2013, 15, 57–65.

[18] SHOCKEY J.S., VON FRAUNHOFER J.A., SELIGSON D., *A measurement of the coefficient of static friction of human long bones*, Surf. Technol., 1985, 25, 167–173.

[19] THUR C.K., EDGREN G., JANSSON K.A., WRETENBERG P., *Epidemiology of adult ankle fractures in Sweden between 1987 and 2004: a population-based study of 91,410 Swedish inpatients*, Acta Orthop., 2012, 83, 276–281.

[20] VLCEK M., LANDOR I., HORAK Z., MUSIL V., SOSNA A., JONAS D., *Mathematical modelling for the comparison of plate and intramedullary osteosynthesis stability in intraarticular distal radius fractures*, Bratisl. Lek Listy, 2014, 115, 107–111.

[21] WENDSCHE P., DRAC P., *Are malleolar fractures easy to treat?*, Acta Chir. Orthop. Traumatol. Cech., 2012, 79, 540–548.

[22] YDE J., *The Lauge Hansen classification of malleolar fractures*, Acta Orthop. Scand., 1980, 51, 181–192.